ORIGINAL ARTICLE

Proteomics of colorectal cancer liver metastasis: A quantitative focus on drug elimination and pharmacodynamics effects

Areti-Maria Vasilogianni[1] | Zubida M. Al-Majdoub[1] | Brahim Achour[1] |
Sheila Annie Peters[2] | Amin Rostami-Hodjegan[1,3] | Jill Barber[1]

[1]Centre for Applied Pharmacokinetic Research, School of Health Sciences, The University of Manchester, Manchester, UK

[2]Translational Quantitative Pharmacology, Merck KGaA, Darmstadt, Germany

[3]Certara Inc (Simcyp Division), Sheffield, UK

Correspondence
Jill Barber, Centre for Applied Pharmacokinetic Research, School of Health Sciences, The University of Manchester, Stopford Building, Oxford Road, Manchester, M13 9PT, UK.
Email: jill.barber@manchester.ac.uk

Funding information
Merck KGaA

Aims: This study aims to quantify drug-metabolising enzymes, transporters, receptor tyrosine kinases (RTKs) and protein markers (involved in pathways affected in cancer) in pooled healthy, histologically normal and matched cancerous liver microsomes from colorectal cancer liver metastasis (CRLM) patients.

Methods: Microsomal fractionation was performed and pooled microsomes were prepared. Global and accurate mass and retention time liquid chromatography–mass spectrometry proteomics were used to quantify proteins. A QconCAT (KinCAT) for the quantification of RTKs was designed and applied for the first time. Physiologically based pharmacokinetic (PBPK) simulations were performed to assess the contribution of altered abundance of drug-metabolising enzymes and transporters to changes in pharmacokinetics.

Results: Most CYPs and UGTs were downregulated in histologically normal relative to healthy samples, and were further reduced in cancer samples (up to 54-fold). The transporters, MRP2/3, OAT2/7 and OATP2B1/1B3/1B1 were downregulated in CRLM. Application of abundance data in PBPK models for substrates with different attributes indicated substantially lower (up to 13-fold) drug clearance when using cancer-specific instead of default parameters in cancer population. Liver function markers were downregulated, while inflammation proteins were upregulated (by up to 76-fold) in cancer samples. Various pharmacodynamics markers (e.g. RTKs) were altered in CRLM. Using global proteomics, we examined proteins in pathways relevant to cancer (such as metastasis and desmoplasia), including caveolins and collagen chains, and confirmed general over-expression of such pathways.

Conclusion: This study highlights impaired drug metabolism, perturbed drug transport and altered abundance of cancer markers in CRLM, demonstrating the importance of population-specific abundance data in PBPK models for cancer.

KEYWORDS
colorectal cancer liver, metastasis, drug-metabolizing enzymes, inflammation, metastasis, PBPK, proteomics, QconCAT, receptor tyrosine kinases, transporters

1 | INTRODUCTION

Colorectal cancer (CRC) is the third most common type of cancer worldwide,[1] with half of patients having liver metastasis.[2] Surgical resection is the ideal intervention for colorectal cancer liver metastasis (CRLM), but this is not always possible and other adjuvant therapies (e.g. chemotherapy) are available.[3] Because liver metastasis is common, pharmacokinetics (PK) of many drugs differ in CRC patients due to perturbed system parameters.[4–8] Despite the fact that a constant dosage is often used throughout the cancer chemotherapy, there are temporal changes in pharmacodynamic (PD) targets with disease progression or remission. The proteomic nature of these changes has not been well studied with respect to altered expression of drug targets during cancer progression,[9] which has been reported across different cancer types.[10]

To translate the effects of changes in expression under disease conditions to in vivo outcomes, proteomics data are used within the framework of in vitro to in vivo extrapolation linked to physiologically based PK (PBPK)/PD modelling.[11,12] However, protein abundance data are limited in cancer populations. The limited qualitative data available on CRLM on the expression of drug-metabolising enzymes (DMEs)[13] suggest that cancer may alter drug metabolism. Quantitative transporter data in CRLM are limited to mRNA measurements[14] or comparison of expression in livers from healthy donors with that in histologically normal livers from CRLM patients.[15] Expression of pharmacodynamic targets including receptors is also affected by cancer. Of particular interest are receptor tyrosine kinases (RTKs), which regulate cellular processes and many anticancer drugs, such as regorafenib, inhibit them, thus improving survival of CRLM patients.[16,17] RTK mRNA and protein expression data have been measured in cell lines[18–20] but human studies are only limited to immunohistochemistry.[21–24]

This study, therefore, aimed to apply global and QconCAT-based proteomics to quantify PK and PD proteins in pooled liver samples from healthy (healthy donors), histologically normal (peri-carcinomatous) and matched cancerous liver tissue from CRLM patients. The target proteins are involved in drug metabolism, transport and pathways affected in cancer. Notably, we designed, for the first time, a QconCAT standard (KinCAT) for absolute quantification of RTKs. We additionally assessed the contribution of altered abundance using PBPK models. The generated abundance data will fill key gaps in current knowledge about human enzymes, transporters and PD targets in CRLM.

2 | METHODS

2.1 | Liver samples and donor characteristics

Matched cancerous and histologically normal liver tissues from adult CRLM patients were supplied by the Manchester University NHS Foundation Trust (MFT) Biobank, Manchester, UK, following hepatectomy. Ethics were covered under the MFT Biobank generic

---

What is already known about this subject

- Enzymes and transporters are perturbed in different cancer types, and thus, pharmacokinetics of drugs is affected in cancer patients.
- Various pharmacodynamic markers and targets involved in biological pathways are also affected.
- Quantitative perturbation data are not available for colorectal cancer liver metastases (CRLM).

What this study adds

- Expression of proteins involved in liver drug metabolism and disposition is impaired in CRLM.
- Expression of pharmacology markers (e.g., receptor tyrosine kinases) changes in CRLM, leading to perturbations in biological pathways (metastasis and angiogenesis).
- Altered abundance of enzymes and transporters affects predicted drug clearance in CRLM patients.

---

ethical approval (NRES 14/NW/1260 and 19/NW/0644). Healthy human liver microsomal samples (tumour-free) from healthy subjects were collected postmortem and provided by Pfizer (Groton, CT, USA), and prepared previously by Vitron (Tucson, AZ, USA) and BD Gentest (San Jose, CA, USA). Ethical approval was obtained by the suppliers. Tables S1 and S2 present demographic and clinical information.

2.2 | QconCATs standards

MetCAT and TransCAT standards have been used in this study, as described previously.[25,26] A modified version of the TransCAT was used (Supplementary Information). KinCAT is a novel QconCAT for the quantification of human RTKs. It consists of concatenated tryptic peptides representative of the following proteins: macrophage colony-stimulating factor 1 receptor (CSF1R), epidermal growth factor receptor (EGFR), ephrin type-A receptor 2 (EPH2A), erythroblastic oncogene B2 (ERBB2), fibroblast growth factor receptors (FGFR1/2/3), FMS-like tyrosine kinase (FLT3), insulin-like growth factor 1 receptor (IGF1R), insulin receptor (INSR), mast/stem cell growth factor receptor (KIT), hepatocyte growth factor receptor (MET), neurotrophic tyrosine kinase receptor type 2 (NTRK2), platelet-derived growth factor receptors (PGFRA/B), proto-oncogene tyrosine-protein kinase receptor (RET), angiopoietin-1 receptor (TIE2), tyrosine-protein kinase receptor UFO (AXL), vascular endothelial growth factor receptors (VGFR1/2/3). These proteins were selected for their crucial role
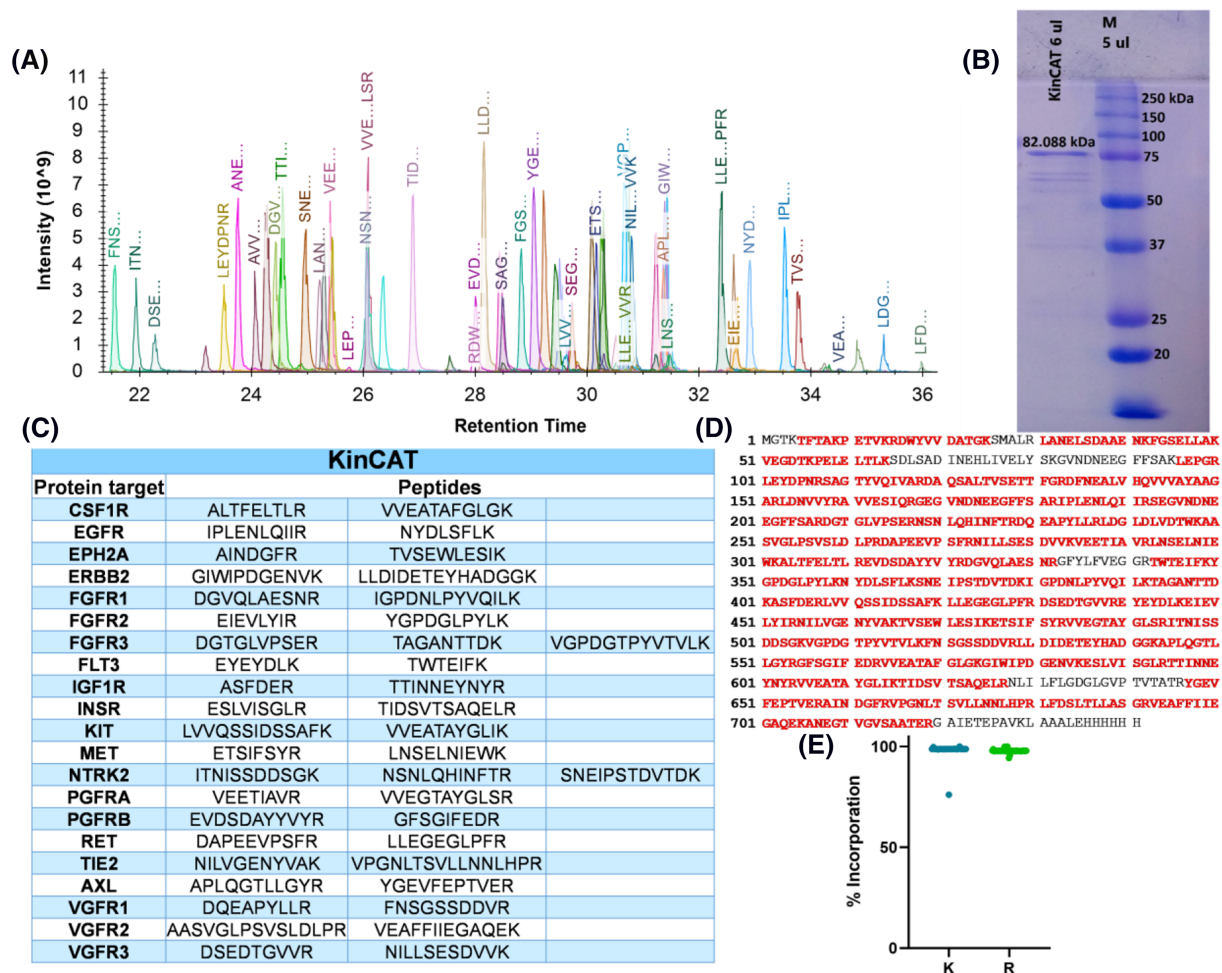
FIGURE 1 Design and characterization of the KinCAT. Liquid chromatography–mass spectrometry traces of peptides included in the KinCAT sequence (A). SDS-PAGE gel showing the expression and purity of KinCAT; M = molecular weight marker (B). Sequences of KinCAT peptides and the RTK proteins they represent (C). Sequence coverage of the KinCAT protein, showing complete expression (D). Incorporation efficiency of $^{13}C_6$-lysines (K) and arginines (R) in the KinCAT peptides (E)

in cancer biology and treatment. Details are provided in Supplementary Information and Figure 1.

2.3 | Sample preparation for proteomics

Liver tissue samples were fractionated to microsomes,[8] as described in Supplementary Methods. Pooled samples were made up by combining equal volumes of individual microsomes from either 15 healthy samples (HP), 16 histologically normal samples (NP) from CRLM patients or 16 matched cancerous liver samples (TP) from the same CRLM patients. Each pooled sample (70 μg) was spiked with known amounts (Supplementary Methods) of each isotopically-labelled QconCAT, and prepared using filter-aided sample preparation.[27–29] Samples were denatured (sodium dexoycholate, 10% w/v final concentration), reduced (dithiothreitol, 0.1 M final concentration), alkylated (iodoacetamide, 100 μL of 50 mM) and digested (2 doses of

LysC 2% w/w, 30°C, 4 h, and trypsin 4% w/w, 37°C, 16 h).[30] Unlabelled peptide standards, GVNDNEEGFFSAR, VGFLPDGVIK and SEGVNDNEEGFFSAR, were added to quantify the QconCATs (MetCAT, TransCAT and KinCAT, respectively). Samples were lyophilized by vacuum centrifugation after sample preparation and stored at −20°C until mass spectrometric (MS) analysis. Additional details are provided in Supplementary Methods.

2.4 | Liquid chromatography and tandem MS

Dried samples were re-suspended (3% acetonitrile-0.1% formic acid) and loaded onto an UltiMate 3000 Rapid Separation liquid chromatography (LC) system (Dionex Corporation, Sunnyvale, CA, USA) coupled to a Q Exactive HF Hybrid Quadrupole-Orbitrap MS (Thermo Fisher Scientific, Waltham, MA, USA). Details are provided in Supplementary Methods.

2.5 | Analysis and annotation of proteomic data

Proteomic data were processed using MaxQuant 1.6.7.0 (Max Planck Institute, Martinsried, Germany), and searched against a customized database, comprising human UniprotKB database (74 788 sequences) and QconCAT sequences. For targeted accurate mass and retention time (AMRT) analysis, light-to-heavy intensity ratios were used with QconCAT concentrations to calculate protein amounts based on accurate mass and retention time for each peptide.[27,31] Peptides selected for quantification of CYPs/UGTs, transporters and RTKs are presented in Tables S6, S7 and S8, respectively. For global analysis, data were processed using the total protein approach (TPA) based on the ratio of individual protein to total proteome MS signal intensity.[32]

2.6 | Physiologically-based pharmacokinetic (PBPK) simulations

The effect of abundance of DMEs and transporters on simulated plasma drug clearance was assessed using PBPK modelling on Simcyp V20 Release 1 (Certara, Sheffield, UK) on 50 substrates with different attributes and hepatic extraction ratios. The compound files were available in Simcyp library (Table S5), and PBPK simulations used system parameters available on the simulator for healthy and cancer populations. The effects of abundance changes (based on TPA) in CRLM were assessed using previously described models[8]:

Model 1 (Healthy): default microsomal protein per gram of liver (MPPGL) and abundance levels for the healthy population (Simcyp).
Model 2 (Cancer-D): default MPPGL and abundance for the cancer population (Simcyp).
Model 3 (New Cancer-ALN): MPPGL of histologically normal tissue[8] and abundances of DMEs and transporters in histologically normal relative to healthy tissue were used for the cancer population, assuming the whole liver is histologically normal (maximum metabolic capacity).
Model 4 (New Cancer-ALC): MPPGL of cancerous tissue[8] and abundance of DMEs and transporters in tumour relative to healthy tissue were used for the cancer population, assuming the whole liver is cancerous (minimum metabolic capacity) and liver mass is unchangeable.

The relative ratios of the clearance (CL) were compared.

2.7 | Data analysis

Ratios were calculated for abundances in histologically normal and tumour samples relative to healthy control samples. Expression levels with ratios within 2-fold (0.5–2.0) were considered similar. Graphs were generated using GraphPad Prism 8.1.2 (GraphPad Software, La Jolla, CA, USA).

2.8 | Nomenclature of targets and ligands

Key protein targets and ligands in this article are hyperlinked to corresponding entries in http://www.guidetopharmacology.org, and are permanently archived in the Concise Guide to PHARMACOLOGY 2019/20.[33,34]

3 | RESULTS

All results were based on 3 pooled samples made up of healthy, histologically normal and tumour tissue. Each measurement was duplicated and found to be consistent (within a factor of 2 in all but 3 cases of enzymes; Table S9). A single value-not an average is reported here.

3.1 | Novel QconCAT (KinCAT) for the quantification of kinases

Kinases regulate cellular processes and are involved in the development and progression of cancer. Kinase expression has not previously been quantified by mass spectrometry-based methods in human tissue. We have therefore designed a QconCAT (KinCAT) to quantify RTKs (Figure 1A and C). The KinCAT, including N-terminal core ribosomal protein to improve expression of the KinCAT[30] with a histidine tag for purification, migrated on SDS-PAGE (molecular mass 82 kDa), demonstrating that the intact QconCAT was expressed (Figure 1B). This was confirmed by Mascot sequence coverage (88%; Figure 1D). The ^{13}C-labelling efficiency was >97% (Figure 1E). The LC–MS traces of the digested KinCAT peptides are shown in Figure 1A, using Skyline (version 19.01.193; www.sciex.com/products/software/skyline-software). More details about the KinCAT are provided in the Table S4.

3.2 | Abundance of enzymes and transporters in healthy, histologically normal, and cancerous liver

3.2.1 | Absolute abundance of CYP and UGT enzymes

The effect of cancer on the expression of DMEs was evaluated by comparing the expression in 1 pooled healthy (HP), 1 pooled histologically normal (NP) and 1 pooled tumorous sample (TP) from CRLM patients using accurate mass and retention time. With the exception of CYP2J2, protein expression of CYPs (Figure 2A) and UGTs (Figure 2D) in healthy tissue is similar to that in normal. Abundances of CYPs and UGTs in HP ranged from 0.16 to 90.2 and 7.7 to 60.7 pmol/mg microsomal protein, respectively. Interestingly, enzyme expression was significantly decreased for all CYPs and UGTs in tumour (Figure 2A and D). In healthy tissue, the most abundant CYPs are reported to be CYP2E1 and CYP3A4[28] as here.
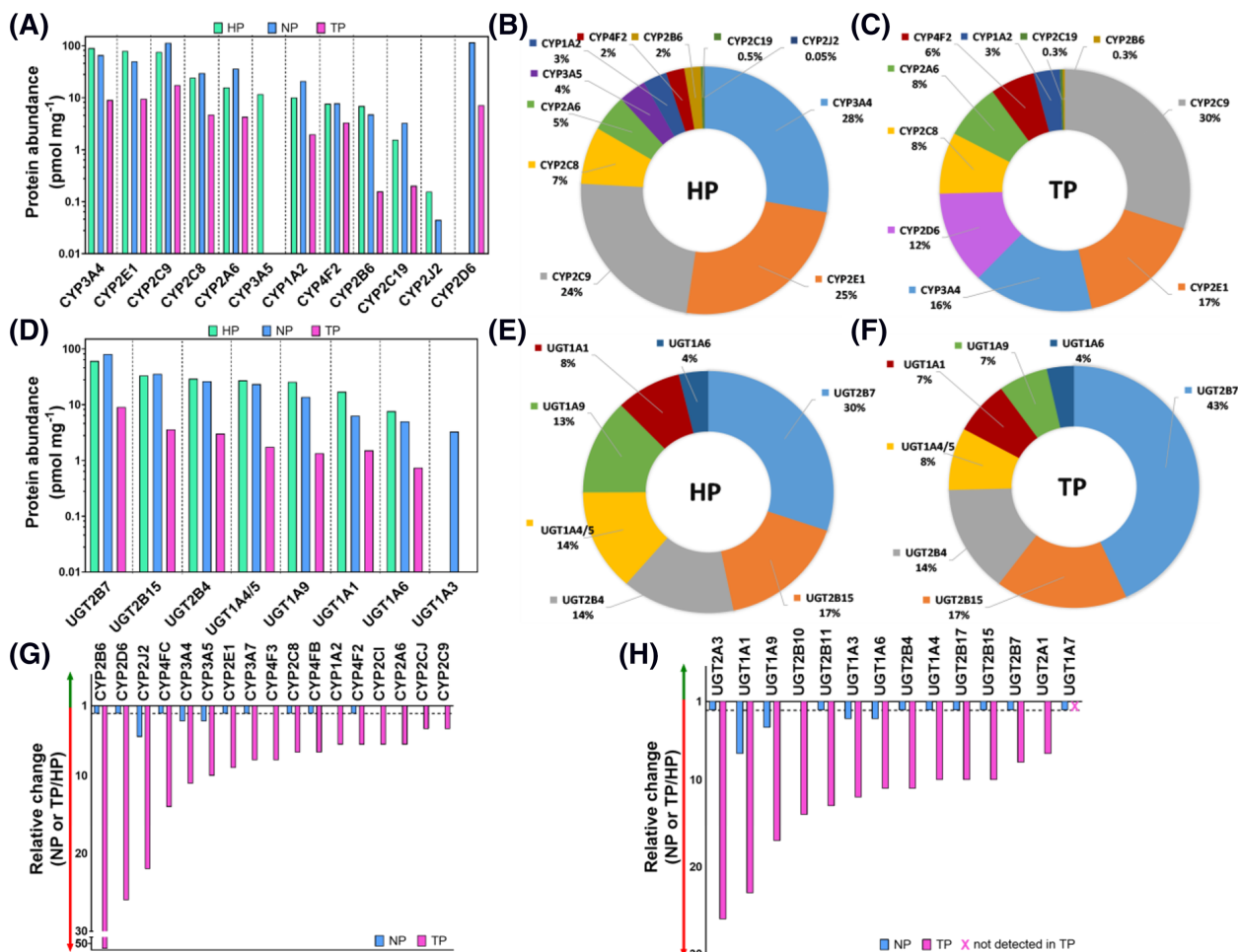
FIGURE 2   Protein expression of cytochrome P450 enzymes (CYPs) and UDP-glucuronosyltransferases (UGTs) in healthy (HP), histologically normal (NP) and tumorous (TP) pooled hierarchical linear modelling samples. Absolute abundance of CYPs (A) and UGTs (D) is expressed in pmol/ mg of microsomal protein. Pie charts represent the distribution of CYPs (B, C), and UGTs (E, F) in HP and TP, respectively, based on their absolute abundance. The relative changes in expression of CYPs (G) and UGTs (H) in NP and TP compared with HP. The green and red arrows indicate increased and decreased expression relative to HP, respectively. The dotted line represents 2-fold change

Interestingly, **CYP2C9** was the most abundant (17.4 pmol/mg microsomal protein) in tumour, followed by 2E1, and 3A4 (9.5 and 9 pmol/mg, respectively). The most abundant UGT was UGT2B7 in all samples but whereas histologically normal tissue showed 80.9 pmol/mg and healthy 60.7 pmol/mg, this fell to 9.1 pmol/mg in tumour. **CYP2D6**, UGT1A3 and CYP3A5 were not detected in all samples in the targeted analysis so are discussed below in TPA analysis.

3.2.2 | Abundance distribution of CYPs and UGTs in HP and TP

The pie charts in Figure 2 represent the abundance distribution (based on targeted analysis) of CYPs (Figure 2B and C) and UGTs (Figure 2E and F) in HP and TP. This visualization clearly shows the dominance of CYP2C9 (30%) in tumour against CYP3A4 (28%) in healthy tissue.

3.2.3 | Fold change in the expression of CYPs and UGTs in TP and NP relative to HP

The targeted approach is generally considered to be the gold standard in accuracy but is restricted to proteins for which both standard and analyte are detected. We therefore further analysed the data using the total protein approach, which is untargeted. In Figure 2G and H, the abundances of enzymes in NP and TP are expressed relative to HP. Most of the CYPs in NP were within 2-fold of levels in HP, except CYP3A4 and CYP3A5 (3-fold lower in NP), and CYP2J2 (5-fold lower in NP). Most of UGTs however were downregulated by more than 2-fold (up to 7-fold for **UGT1A1**) in NP. Both CYPs and UGTs were dramatically downregulated in tumour ranging from 4 (CYP2C9) to 54-fold (**CYP2B6**).

The relative quantification by the 2 methods was in broad agreement. The TPA permits the quantification of many more proteins at the expense of the precision we obtain with the targeted approach.

3.2.4 | Abundance of transporters in healthy, histologically normal and cancerous liver

Expression of ABC and SLC transporters, plasma membrane protein (ATP1A1) and cadherin-like transporter (CDH17) was measured using AMRT targeted method (Figure 3A and B). The QconCAT permits the quantification of 7 ABC transporters, which were detected in healthy and histologically normal samples. BCRP, MRP6 and BSEP fell below the limit of quantification in tumour and 3 others (MDR3, MRP2 and MRP3) were also much reduced (Figure 3A). P-gp alone of the ABC transporters rose in TP (0.71 and 0.46 pmol/mg protein in TP and HP). ATP1A1 was moderately abundant in healthy liver, as indicated previously,[28] and its abundance was higher in cancer (16.3 pmol/mg in TP and 7.3 pmol/mg in HP). CDH17 was only quantifiable in NP and TP. Expression of SLCs was perturbed in cancer, with significantly lower abundance of OAT7, OATP2B1, OATP1B3, OATP1B1 and OAT2 in TP (0.25, 0.69, 0.36, 0.54 and 0.16 pmol/mg, respectively) compared with HP (3.3, 2.4, 2.4, 2.0 and 1.5 pmol/mg, respectively).

### 3.2.5 | Untargeted relative quantification of transporters

The TPA is able to quantify OCT3 and MRP4 for which there were no standards (Figure 3C and D). MRP4 was hardly changed, but OCT3 was significantly reduced in cancer. As expected, the other transporters followed the same trends as the targeted analysis.

3.2.6 | Differential protein abundance of non-CYP non-UGT and antioxidant enzymes

Figure 4A and B depict the relative changes in abundance of non-CYP non-UGT DMEs (for which no labelled standards were available) using the TPA. FMO4, ALDH2, SULT1A2, SULT1B1, ADH4, ADH6, ADH1B and AOXA were more abundant in NP compared with HP, whereas CES3, POR, MGST2 and MGST3 were less abundant (>2-fold change). The suppressive effect of cancer on expression was observed with CES1/2, FMO3/5, MGST1/2/3, POR, MGST1/2/3, ALDH1A/1G,
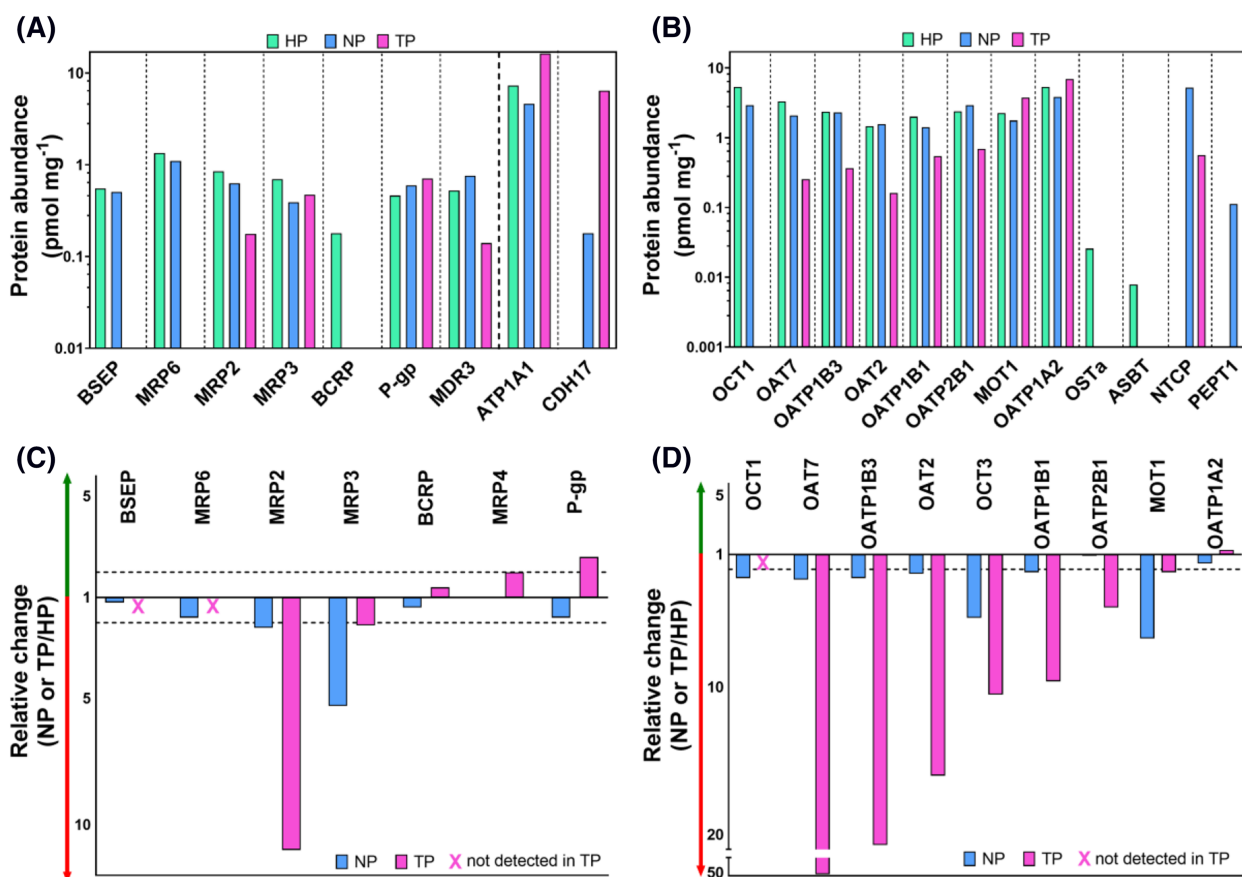
FIGURE 3 Abundance of transporters in healthy (HP), histologically normal (NP) and tumorous (TP) pooled hierarchical linear modelling samples. Absolute abundance of ABC transporters, plasma membrane marker (ATP1A1) and 1 adhesion protein (CDH17; A) and solute carriers (SLCs; B), expressed in pmol of protein/mg of total protein. Relative change in expression of ABC (C) and SLC (D) transporters in NP and TP, compared with HP. The green and red arrows indicate increased and decreased expression relative to HP, respectively. The dotted line represents 2-fold change
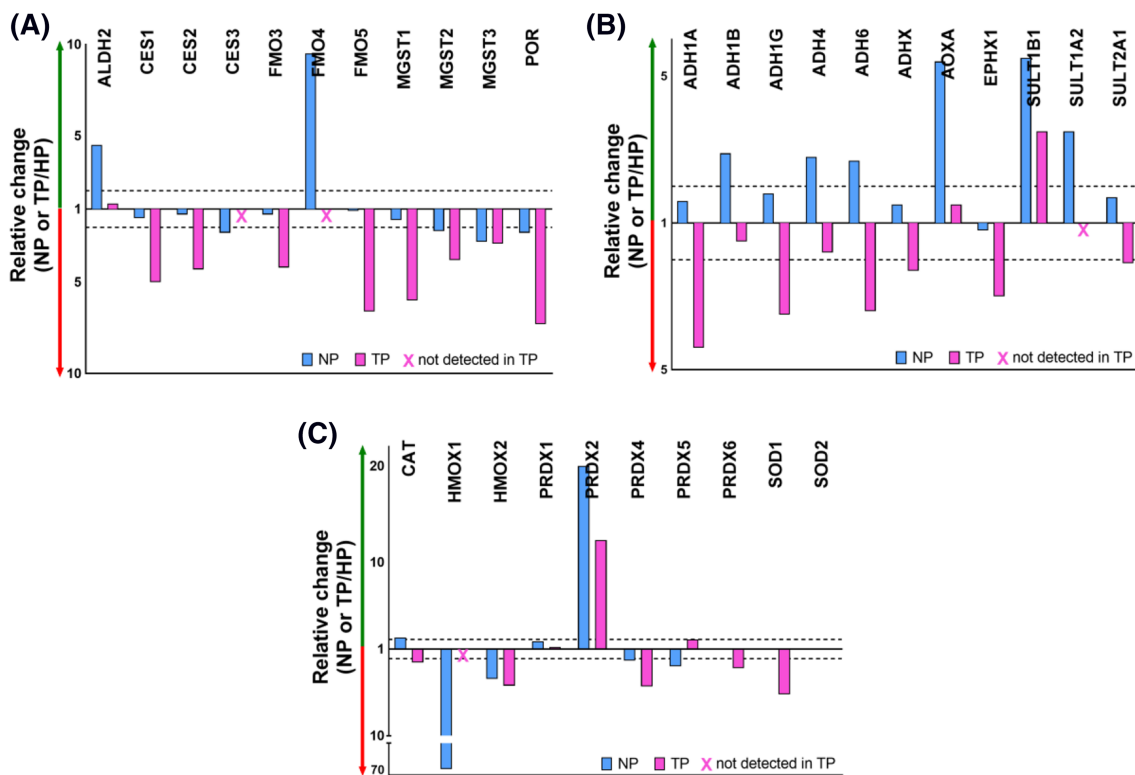
FIGURE 4 Relative abundance of non-CYP non-UGT enzymes (A, B), and antioxidant enzymes (C) measured in healthy (HP), histologically normal (NP) and tumorous (TP) pooled hierarchical linear modelling samples. The green and red arrows indicate higher or lower expression relative to HP, respectively. The dotted line is set to 2-fold change. (A) ALDH, aldehyde dehydrogenase; CES, carboxylesterase; FMO, flavin-containing monooxygenase; MGST, microsomal glutathione S-transferase; POR, NADPH-cytochrome P450 reductase. (B) ADH, alcohol dehydrogenase; AOX, aldehyde oxidase; EPHX, epoxide hydrolase; SULT, sulfotransferase. (C) CAT, catalase; HMOX, haem-oxygenase; PRDX, peroxiredoxin; SOD, Superoxide dismutase

ADH6, ADHX, EPHX1 and SULT2A1, with up to 7.3-fold lower levels (tumour vs. healthy).

The abundances of antioxidant enzymes are summarised in Figure 4C. Haem-oxygenase 1 (HMOX1) was observed at 70-fold lower abundance in histologically normal samples compared with healthy and was below the limit of quantification in the tumour. By contrast, peroxiredoxin PRDX2 was expressed at higher levels in normal (20-fold) and tumour (>12-fold) livers compared with healthy. HMOX1 catabolizes haem, and has antiapoptotic and anti-inflammatory functions.[35] PRDX2 induces cancer cell proliferation and protects from reactive oxygen species-induced cell damage and apoptosis.[36]

3.3 | Assessment of changes in expression of kinases in normal and tumour compared with healthy tissue

3.3.1 | Expression levels of receptor tyrosine kinases

To assess the expression of RTKs, AMRT targeted analysis using KinCAT was carried out (Figure 5A). Expression of VGFR1, TIE2,

FGFR3, ERBB2 and IGF1R was higher in NP relative to HP, whereas AXL and VGFR3 were less abundant in NP, and RET was exclusively detected in NP (at 0.04 pmol/mg protein). Compared with HP, expression levels of INSR, EGFR and AXL were lower, and those of NTRK2, ERBB2 and IGF1R were higher in TP. KIT was only expressed in NP and TP. FGFR1 (0.01 pmol/mg), VGFR2 (0.02 pmol/mg), FGFR2 (0.04 pmol/mg), and PGFRB (3.8 pmol/mg) were exclusively detected in TP.

3.3.2 | Other kinases exclusively detected in tumour

Figure 5B shows additional kinases involved in various biological pathways that were exclusively detected in TP, including creatine kinases, mitogen-activated protein kinase, STRAP, PAK1 and GAK.

3.3.3 | Fold change in expression of RTKs between HP to NP and TP

Fold changes in the abundance of RTKs were assessed by the TPA (Figure 5C). The most striking results were: (i) raised levels of KIT,
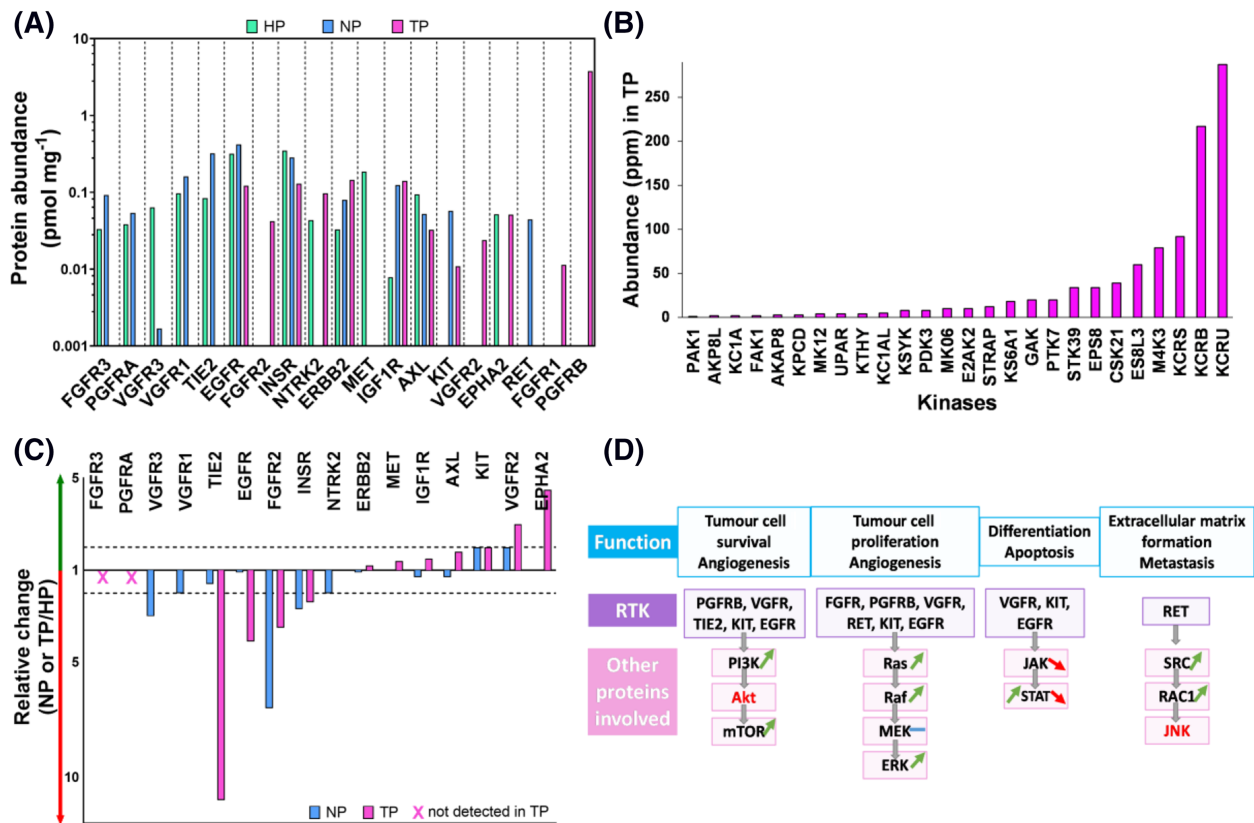
FIGURE 5 Abundance of kinases in healthy (HP), histologically normal (NP) and tumorous (TP) pooled hierarchical linear modelling. (A) Absolute abundance of receptor tyrosine kinases (RTKs), expressed in pmol of protein/mg of liver microsomal protein using KinCAT as standard. (B) Relative abundance of kinases (not RTKs) exclusively identified in TP, expressed as ppm (parts/million) using the total protein approach. (C) Relative change of RTKs in NP and TP compared with HP. When a bar is not present, this means that there was no change in NP or TP compared with HP. The crosses indicate the absence of a protein from a sample. The green and red arrows indicate increased and decreased expression relative to HP, respectively. The dotted line is set to 2-fold change. (D) Functions of RTKs (targeted by anticancer tyrosine kinase inhibitors, TKIs) and biological pathways that are affected by the altered abundances of RTKs. Green and red arrows show increased and decreased abundance of proteins in TP, respectively. The blue line represents exclusive expression (low) in HP, and red font means the target was not detected in any of the samples

VGFR2 and EPHA2 in tumour relative to both histologically normal and healthy; and (ii) decreased levels of TIE2, EGFR, FGFR2 and INSR in tumour. The pattern of expression in histologically normal tissue is less clear-cut for these but in all cases was decreased relative to healthy.

3.3.4 | RTK-related pathways affected in cancer

Figure 5D summarizes the roles of RTKs in terms of functional pathways (tumour cell survival/proliferation, angiogenesis, differentiation/apoptosis, and extracellular matrix formation/metastasis). There is evidence of increased expression of non-RTKs related to cell survival and proliferation and extracellular matrix formation. Interestingly, STAT1 increases, and STAT3/6 decrease in tumour—both these proteins are involved in differentiation and apoptosis. Overall, proteins involved in tumour cell survival, proliferation and metastasis were dysregulated in cancerous livers.
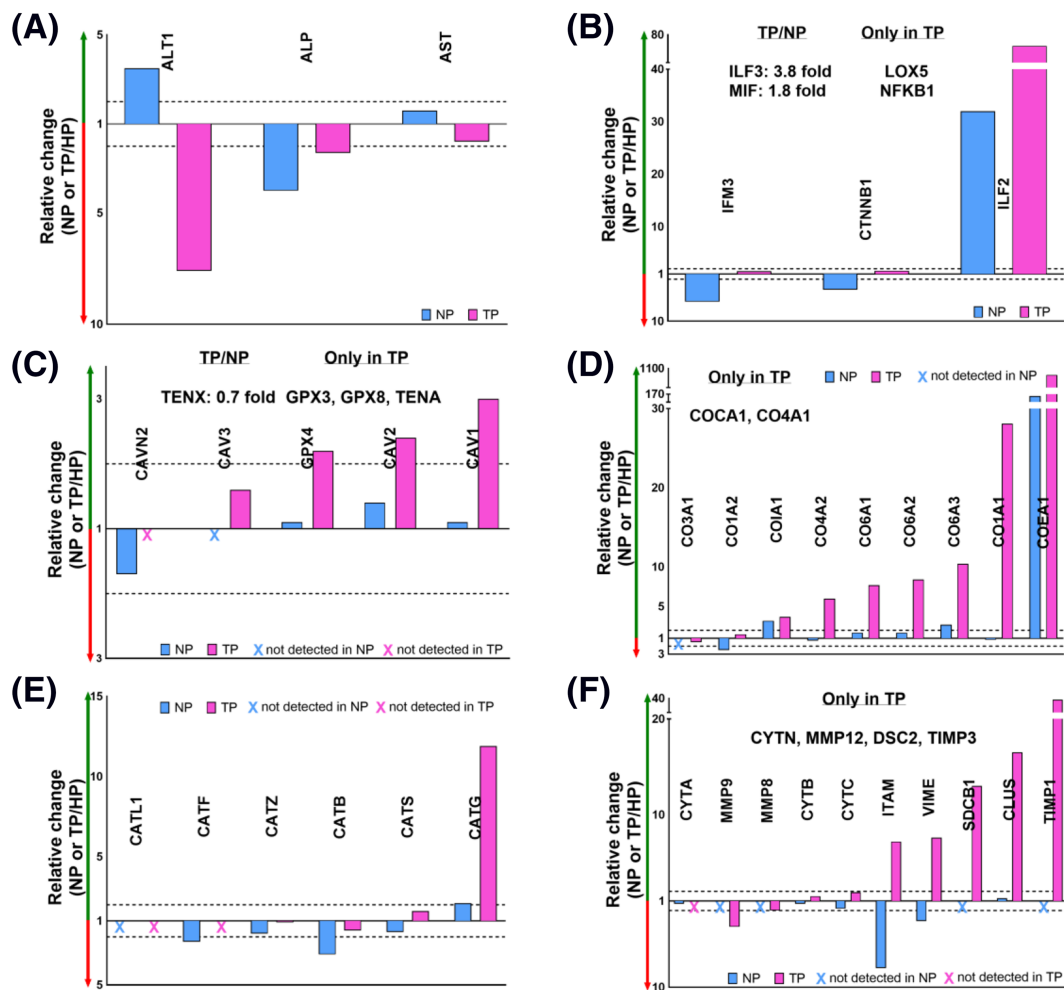
3.4 | Abundance of markers of liver function, inflammation, desmoplasia (fibrosis) and metastasis

By applying the TPA, we assessed fold changes in the abundance of various markers of liver function and conditions induced by cancer in NP and TP relative to HP.

3.4.1 | Liver function

The liver function markers alanine aminotransferase, alkaline phosphatase and aspartate aminotransferase are reported to be increased in the plasma in many cancer patients.[37] Figure 6A shows that in livers all 3 appeared to be decreased (up to 7.6-fold). This may suggest enhanced secretion rather than enhanced production of these markers in cancer.

FIGURE 6 Relative change of markers of liver function (A), inflammation (B), desmoplasia (C), collagen chains (metastasis markers; D), cathepsins (metastasis markers; E), and other metastasis markers (F) in histologically normal (NP) and tumorous (TP) compared with healthy (HP). HP is set to 1 and NP and TP are expressed as relative changes to HP. When a bar is not present, this means that there was no change of expression in NP or TP relative to HP. The crosses indicate absence of a protein from a sample. The green and red arrows indicate increased and decreased expression relative to HP, respectively. The dotted line is set to 2-fold change

3.4.2 | Inflammation

Figure 6B shows modest changes in interferon-induced transmembrane protein 3 and catenin β-1 but huge upregulation of interleukin enhancer-binding factor-2: 76-fold in tumour and above 30-fold in histologically normal adjacent to tumour. interleukin enhancer-binding factor-3, macrophage migration inhibitory factor, arachidonate 5-lipoxygenase and nuclear factor-κB were detected in tumour but below the limit of detection in healthy tissue.

3.4.3 | Desmoplasia

We also measured desmoplasia markers (Figure 6C) involved in the growth of fibrous tissue. Consistent with fibrotic appearance of the tumorous samples observed during tissue fractionation, we detected

glutathione peroxidase (GPX)3, GPX8 and tenascin exclusively in TP. Additionally, GPX4 and caveolins1 and 2 were expressed at higher levels (>2-fold) in TP compared with HP.

3.4.4 | Metastasis markers

Expression of metastasis markers was perturbed in CRLM. As expected, collagen chains were massively upregulated in the tumour samples (Figure 6D)—COIA1 and COEA1 were >1000-fold higher than in the healthy samples and COCA1 and COC4A1 were undetectable in the healthy samples. Interestingly, the histologically normal samples also showed high levels of COIA1 and COEA1—165 times the levels observed in the healthy samples. Cathepsins (Figure 6E) were generally unchanged across all samples, with only CATG being significantly higher (9.9-fold) in TP relative to HP. Other

metastasis markers were also significantly upregulated in tumour samples (see Figure 6F). These proteins have proteolytic function, facilitating matrix degradation and tumour cell invasion.

3.5 | PBPK simulations

The Simcyp simulator contains PBPK models for various drugs in healthy and disease populations. The cancer population is not well defined and systems data such as measured here could improve these models. MPPGL data were previously used to update current PBPK models.[8] In addition to the MPPGL data, abundance data obtained here were used to refine the Simcyp PBPK models. Simulations for 50 substrates with different attributes and hepatic extraction ratios were performed (Figure 7). Four populations were used: the default healthy and cancer populations, and 2 constructed using the data obtained here. New Cancer-ALN uses data from the histologically normal sample assuming the data apply to the whole liver. New Cancer-ALC similarly uses data pertaining to the tumour sample. Ratio of the clearance predicted using New Cancer-ALC was >2-fold lower (up to

13-fold) than that obtained using the default Cancer-D model for 33 out of 50 drugs simulated.

4 | DISCUSSION

For the first time, this study applied targeted and global LC–MS/MS-based proteomics to quantify DMEs, transporters and PD targets (including RTKs, inflammatory markers, metastatic markers) in healthy, histologically normal and cancerous livers from CRLM patients. For the proteins investigated here, no quantitative data have been reported previously in CRLM. Our experimental data were used to optimise PBPK models in cancer population (Simcyp) in order to assess the impact of the changes in abundance on PK.

CYPs and UGTs were significantly downregulated in cancer tissue, highlighting that the clearance of CYP-substrates may be significantly lower in patients with late-stage liver cancer. Abundances of CYPs and UGTs were also lower in histologically normal tissue, meaning that the impact of cancer is not limited to the tumour, but affects the metabolic function of a larger amount of the liver. Additional DMEs such as
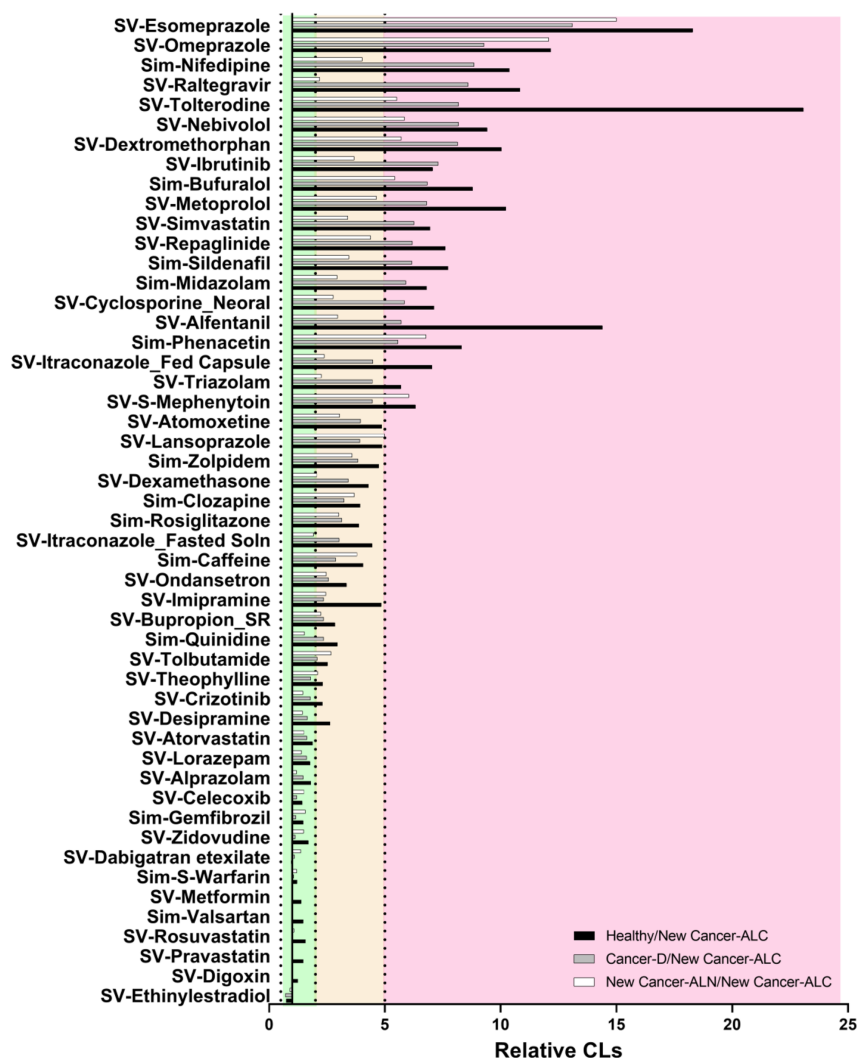
FIGURE 7 Relative ratios of the clearance (CLs) of drugs in Healthy (black), Cancer-D (grey) and New Cancer-ALN (white) to New Cancer-ALC populations. Healthy: default abundances of enzymes and transporters (Simcyp) with a healthy population. Cancer-D: default abundances of enzymes and transporters (Simcyp) with a cancer population. New Cancer-ALN: abundance of enzymes and transporters measured in this study for histologically normal tissue with a cancer population. New Cancer-ALC: abundances of enzymes and transporters measured in this study for cancer tissue with a cancer population. The green rectangle shows the drugs with <2-fold change in drug CL than that obtained using the New Cancer-ALC model, the amber shows 2–5-fold higher CL than that obtained using the New Cancer-ALC model, and the red shows >5-fold higher CL than that obtained using the New Cancer-ALC model

ADHs and FMO3 were downregulated in tumorous tissue, suggesting impaired capacity in almost all drug clearance pathways. Expression of antioxidant enzymes was decreased in tumours and adjacent, histologically normal tissue, suggesting impaired detoxification in CRLM. In agreement with our findings, proteomics and activity data from hepatocellular carcinoma patients showed a significant impact of cancer on CYPs, UGTs, ADHs, FMO3 and SULTs.[5,38–40]

Transporters are important for the disposition of drugs and the trafficking of nutrients and metabolites. Abundance data on transporters showed significant changes in expression in CRLM, suggesting impaired disposition. The majority of SLC transporters were downregulated in cancerous tissue. Efflux transporters, MRP2 and MRP3, which are involved in drug resistance, were downregulated in histologically normal and tumorous tissue, while other efflux transporters, such P-gp and MRP4, were increased in cancer tissue. This is a preliminary finding, which, if reproduced in individual tumours, could have implications for choice of therapy in CRLM. The lower expression of OATPs and OCT1 is consistent with data from hepatocellular carcinoma patients, whereas changes in BCRP, MRPs and P-gp were not consistent.[7] Such differences are not surprising considering differences in the cancer type. This reflects the need to model each cancer type separately.

The protein expression levels of RTKs is reported for the first time in this study. Our approach employed a novel QconCAT as a standard for these low abundance proteins. However, we also conducted global measurements simultaneously using the TPA for quantification. In general, the targeted measurements are more sensitive and more accurate but restricted to a relatively small number of proteins. In both histologically normal and cancerous tissue from CRLM patients, expression of FGFR2 and INSR was downregulated, while that of KIT and VGFR2 upregulated. TIE2 and EGFR were downregulated and EPHA2 upregulated in cancerous livers. The altered expression of these proteins renders them potential diagnostic or therapeutic biomarkers in CRLM. Platelet-derived growth factor receptor (PGFRB) was highly and exclusively detected in tumorous tissue, consistent with literature suggesting PGFRB is a metastasis marker.[24] Desmoplasia markers were upregulated in CRLM patients, indicating extensive growth of fibrous tissue. Consistent with previous findings,[41] expression of collagen chains was significantly higher in CRLM. The observed perturbations of kinases and cancer-related proteins in CRLM suggests a potential effect on cancer-related pathways, such as cell survival/proliferation, angiogenesis, differentiation and metastasis.[42] In the current study, these markers (such as PI3K, mTOR, Ras, Raf, ERK, SRC and RAC1) were affected in CRLM. As pathophysiological changes can affect protein expression, these proteins can be used as potential markers for monitoring disease prognosis and as therapeutic targets. However, it should be noted that all these targets are measured at the time when the patients were going through surgery: it may be possible using recently described analysis of floating RNA in plasma to plot temporal changes from early diagnosis to the point of patient requiring surgery.[43]

Global proteomic data revealed reduced expression of liver function markers and upregulation of inflammatory markers in cancer.

Arachidonate 5-lipoxygenase and nuclear factor-κB, were exclusively detected in cancer tissue, and these constitute important targets for anti-inflammatory drugs.[44] The severity of inflammation in cancer affects the production of cytokines and increases oxidative stress, which leads to perturbations in proteins involved in drug metabolism and disposition and can subsequently alter drug PK in cancer patients.[45]

To assess the impact of the observed changes in expression of DMEs and transporters on drug PK, we performed PBPK simulations on substrates with different attributes and hepatic extraction levels. Decreased clearance of anticancer drugs in cancer patients has been reported previously.[46–48] In our previous study,[8] we assessed the effect of experimentally-derived MPPGL values in CRLM on PK by optimising and updating an existing cancer population in the Simcyp simulator. In the current study, we further updated the cancer population with abundance data for DMEs and transporters. The changes in abundance levels affected drug clearance for most of the drugs under study. With the assumption that the whole liver is tumorous (New Cancer-ALC model), lower drug clearance was predicted compared with a histologically normal liver (New Cancer-ALN model). The PBPK simulations show that appropriate abundance data in combination with appropriate MPPGL scalar values may improve PK predictions, particularly when used with the appropriate percentage of cancerous liver tissue. Clinical data for the simulated drugs in CRLM were not available and we only assessed the impact of change in abundance of DMEs and transporters on PK. Further simulations could verify these updated PBPK cancer models, when clinical data become available.

In conclusion, our data begin to address key gaps in knowledge about human protein abundance in cancer. DMEs were significantly downregulated and transporters were perturbed in CRLM. In addition, RTKs were altered in CRLM, leading to perturbations in biological pathways relevant to cancer development and progression. These data may be valuable for proposing diagnostic and therapeutic markers. Liver function was also impaired and inflammation markers were upregulated in CRLM. Desmoplasia and metastasis markers were highly expressed in cancer samples. PBPK simulations on 50 substrates revealed lower drug clearance (up to 13-fold) when using cancer population-specific abundance data. Our study suggests that appropriate abundance values for CRLM may be used to refine PK predictions.

COMPETING INTERESTS

The authors have no conflict of interest to declare.

CONTRIBUTORS
Participated in research design: Vasilogianni, Peters, Rostami-Hodjegan, Barber.
Conducted experiments: Vasilogianni.
Performed data analysis: Vasilogianni, Al-Majdoub, Achour, Barber.
Wrote or contributed to the writing of the manuscript: Vasilogianni, Al-Majdoub, Achour, Peters, Rostami-Hodjegan, Barber.

DATA AVAILABILITY STATEMENT
The data that support the findings of this study are available from the corresponding author upon request.

ORCID
Areti-Maria Vasilogianni https://orcid.org/0000-0001-6665-6115
Brahim Achour https://orcid.org/0000-0002-2595-5626

REFERENCES
1. Bray F, Ferlay J, Soerjomataram I, Siegel RL, Torre LA, Jemal A. Global cancer statistics 2018: GLOBOCAN estimates of incidence and mortality worldwide for 36 cancers in 185 countries. *CA Cancer J Clin*. 2018;68(6):394-424. https://doi.org/10.3322/caac.21492
2. Maher B, Ryan E, Little M, Boardman P, Stedman B. The management of colorectal liver metastases. *Clin Radiol*. 2017;72(8):617-625. https://doi.org/10.1016/j.crad.2017.05.016
3. Mitchell D, Puckett Y, Nguyen QN. Literature Review of Current Management of Colorectal Liver Metastasis. *Cureus*. 2019;11:e3940. https://doi.org/10.7759/cureus.3940
4. Cheeti S, Budha NR, Rajan S, Dresser MJ, Jin JY. A physiologically based pharmacokinetic (PBPK) approach to evaluate pharmacokinetics in patients with cancer. *Biopharm Drug Dispos*. 2013;34(3):141-154. https://doi.org/10.1002/bdd.1830
5. Yan T, Gao S, Peng X, et al. Significantly Decreased and More Variable Expression of Major CYPs and UGTs in Liver Microsomes Prepared from HBV-Positive Human Hepatocellular Carcinoma and Matched Pericarcinomatous Tissues Determined Using an Isotope Label-free UPLC-MS/MS Method. *Pharm Res*. 2015;32(3):1141-1157. https://doi.org/10.1007/s11095-014-1525-x
6. Shinko D, Diakos CI, Clarke SJ, Charles KA. Cancer-Related Systemic Inflammation: The Challenges and Therapeutic Opportunities for Personalized Medicine. *Clin Pharmacol Ther*. 2017;102(4):599-610. https://doi.org/10.1002/cpt.789
7. Billington S, Ray AS, Salphati L, et al. Transporter Expression in Noncancerous and Cancerous Liver Tissue from Donors with Hepatocellular Carcinoma and Chronic Hepatitis C Infection Quantified by LC-MS/MS Proteomics. *Drug Metab Dispos*. 2018;46(2):189-196. https://doi.org/10.1124/dmd.117.077289
8. Vasilogianni A-M, Achour B, Scotcher D, et al. Hepatic Scaling Factors for In Vitro–In Vivo Extrapolation of Metabolic Drug Clearance in Patients with Colorectal Cancer with Liver Metastasis. *Drug Metab Dispos*. 2021;49(7):563-571. https://doi.org/10.1124/dmd.121.000359
9. Adeyinka A, Nui Y, Cherlet T, Snell L, Watson PH, Murphy LC. Activated mitogen-activated protein kinase expression during human breast tumorigenesis and breast cancer progression. *Clin Cancer Res*. 2002;8(6):1747-1753. http://www.ncbi.nlm.nih.gov/pubmed/12060612
10. Koivunen J, Aaltonen V, Peltonen J. Protein kinase C (PKC) family in cancer progression. *Cancer Lett*. 2006;235(1):1-10. https://doi.org/10.1016/j.canlet.2005.03.033
11. Prasad B, Vrana M, Mehrotra A, Johnson K, Bhatt DK. The Promises of Quantitative Proteomics in Precision Medicine. *J Pharm Sci*. 2017;106(3):738-744. https://doi.org/10.1016/j.xphs.2016.11.017
12. Rostami-Hodjegan A. Physiologically Based Pharmacokinetics Joined With In Vitro–In Vivo Extrapolation of ADME: A Marriage Under the Arch of Systems Pharmacology. *Clin Pharmacol Ther*. 2012;92(1):50-61. https://doi.org/10.1038/clpt.2012.65
13. Lane CS, Nisar S, Griffiths WJ, et al. Identification of cytochrome P450 enzymes in human colorectal metastases and the surrounding liver: a proteomic approach. *Eur J Cancer*. 2004;40(14):2127-2134. https://doi.org/10.1016/j.ejca.2004.04.029
14. Wlcek K, Svoboda M, Riha J, et al. The analysis of organic anion transporting polypeptide (OATP) mRNA and protein patterns in primary and metastatic liver cancer. *Cancer Biol Ther*. 2011;11(9):801-811. http://www.ncbi.nlm.nih.gov/pubmed/21383546
15. Kurzawski M, Szeląg-Pieniek S, Łapczuk-Romańska J, et al. The reference liver – ABC and SLC drug transporters in healthy donor and metastatic livers. *Pharmacol Rep*. 2019;71(4):738-745. https://doi.org/10.1016/j.pharep.2019.04.001
16. Lee S, Oh SC. Advances of Targeted Therapy in Treatment of Unresectable Metastatic Colorectal Cancer. *Biomed Res Int*. 2016;2016:1-14. https://doi.org/10.1155/2016/7590245
17. García-Aranda M, Redondo M. Targeting Receptor Kinases in Colorectal Cancer. *Cancers (Basel)*. 2019;11(4):433. https://doi.org/10.3390/cancers11040433
18. Kim H-J, Lin D, Lee H-J, Li M, Liebler DC. Quantitative Profiling of Protein Tyrosine Kinases in Human Cancer Cell Lines by Multiplexed Parallel Reaction Monitoring Assays. *Mol Cell Proteomics*. 2016;15(2):682-691. https://doi.org/10.1074/mcp.O115.056713
19. Kao H-W, Chen H-C, Wu C-W, Lin W-C. Tyrosine-kinase expression profiles in human gastric cancer cell lines and their modulations with retinoic acids. *Br J Cancer*. 2003;88(7):1058-1064. https://doi.org/10.1038/sj.bjc.6600821
20. Potratz J, Tillmanns A, Berning P, et al. Receptor tyrosine kinase gene expression profiles of Ewing sarcomas reveal ROR1 as a potential therapeutic target in metastatic disease. *Mol Oncol*. 2016;10(5):677-692. https://doi.org/10.1016/j.molonc.2015.12.009
21. Ljuslinder I, Malmer B, Isaksson-Mettävainio M, et al. ErbB 1-4 expression alterations in primary colorectal cancers and their corresponding metastases. *Anticancer Res*. 2009;29(5):1489-1494. http://www.ncbi.nlm.nih.gov/pubmed/19443355
22. Yao Y-L, Shao J, Zhang C, et al. Proliferation of Colorectal Cancer Is Promoted by Two Signaling Transduction Expression Patterns: ErbB2/ErbB3/AKT and MET/ErbB3/MAPK. *PLoS ONE*. 2013;8(10):e78086. https://doi.org/10.1371/journal.pone.0078086
23. Saito T, Masuda N, Miyazaki T, et al. Expression of EphA2 and E-cadherin in colorectal cancer: correlation with cancer metastasis. *Oncol Rep*. 2004;11(3):605-611. http://www.ncbi.nlm.nih.gov/pubmed/14767510
24. Steller EJA, Raats DA, Koster J, et al. PDGFRB Promotes Liver Metastasis Formation of Mesenchymal-Like Colorectal Tumor Cells. *Neoplasia*. 2013;15(2):204-IN30. https://doi.org/10.1593/neo.121726
25. Harwood MD, Achour B, Russell MR, Carlson GL, Warhurst G, Rostami-Hodjegan A. Application of an LC–MS/MS method for the simultaneous quantification of human intestinal transporter proteins absolute abundance using a QconCAT technique. *J Pharm Biomed Anal*. 2015;110:27-33. https://doi.org/10.1016/J.JPBA.2015.02.043
26. Russell MR, Achour B, McKenzie EA, et al. Alternative fusion protein strategies to express recalcitrant QconCAT proteins for quantitative proteomics of human drug metabolizing enzymes and transporters. *J Proteome Res*. 2013;12(12):5934-5942. https://doi.org/10.1021/pr400279u
27. Al-Majdoub ZM, Al Feteisi H, Achour B, et al. Proteomic quantification of human blood–brain barrier SLC and ABC transporters in

healthy individuals and dementia patients. *Mol Pharm*. 2019;16(3):1220-1233. https://doi.org/10.1021/acs.molpharmaceut.8b01189

28. Couto N, Al-Majdoub ZM, Achour B, Wright PC, Rostami-Hodjegan A, Barber J. Quantification of Proteins Involved in Drug Metabolism and Disposition in the Human Liver Using Label-Free Global Proteomics. *Mol Pharm*. 2019;16(2):632-647. https://doi.org/10.1021/acs.molpharmaceut.8b00941

29. Couto N, Al-Majdoub ZM, Gibson S, et al. Quantitative Proteomics of Clinically Relevant Drug-Metabolizing Enzymes and Drug Transporters and Their Intercorrelations in the Human Small Intestine. *Drug Metab Dispos*. 2020;48(4):245-254. https://doi.org/10.1124/dmd.119.089656

30. Al-Majdoub ZM, Carroll KM, Gaskell SJ, Barber J. Quantification of the proteins of the bacterial ribosome using QconCAT technology. *J Proteome Res*. 2014;13(3):1211-1222. https://doi.org/10.1021/pr400667h

31. Al-Majdoub ZM, Couto N, Achour B, et al. Quantification of Proteins Involved in Intestinal Epithelial Handling of Xenobiotics. *Clin Pharmacol Ther*. 2021;109(4):1136-1146. https://doi.org/10.1002/cpt.2097

32. Al-Majdoub ZM, Achour B, Couto N, et al. Mass spectrometry-based abundance atlas of ABC transporters in human liver, gut, kidney, brain and skin. *FEBS Lett*. 2020;594(23):4134-4150. https://doi.org/10.1002/1873-3468.13982

33. Alexander SPH, Fabbro D, Kelly E, et al. The Concise Guide to PHARMACOLOGY 2019/20: Enzymes. *Br J Pharmacol*. 2019;176:S297-S396. https://doi.org/10.1007/s002800050808

34. Alexander SPH, Kelly E, Mathie A, et al. The Concise Guide to PHARMACOLOGY 2019/20: Transporters. *Br J Pharmacol*. 2019;176:S397-S493. https://doi.org/10.1111/bph.14753

35. Podkalicka P, Mucha O, Józkowicz A, Dulak J, Łoboda A. Heme oxygenase inhibition in cancers: possible tools and targets. *Współczesna Onkol*. 2018;2018(1):23-32. https://doi.org/10.5114/wo.2018.73879

36. Lee KW, Lee DJ, Lee JY, Kang DH, Kwon J, Kang SW. Peroxiredoxin II Restrains DNA Damage-induced Death in Cancer Cells by Positively Regulating JNK-dependent DNA Repair*. *J Biol Chem*. 2011;286(10):8394-8404. https://doi.org/10.1074/jbc.M110.179416

37. Jiang Z, Li C, Zhao Z, et al. Abnormal Liver Function Induced by Space-Occupying Lesions Is Associated with Unfavorable Oncologic Outcome in Patients with Colorectal Cancer Liver Metastases. *Biomed Res Int*. 2018;2018:1-7. https://doi.org/10.1155/2018/9321270

38. Hu H, Ding X, Yang Y, et al. Changes in glucose-6-phosphate dehydrogenase expression results in altered behavior of HBV-associated liver cancer cells. *Am J Physiol Liver Physiol*. 2014;307(6):G611-G622. https://doi.org/10.1152/ajpgi.00160.2014

39. Xie C, Yan T, Chen J, et al. LC-MS/MS quantification of sulfotransferases is better than conventional immunogenic methods in determining human liver SULT activities: implication in precision medicine. *Sci Rep*. 2017;7(1):3858. https://doi.org/10.1038/s41598-017-04202-w

40. Yan T, Lu L, Xie C, et al. Severely Impaired and Dysregulated Cytochrome P450 Expression and Activities in Hepatocellular Carcinoma: Implications for Personalized Treatment in Patients. *Mol Cancer Ther*. 2015;14(12):2874-2886. https://doi.org/10.1158/1535-7163.MCT-15-0274

41. van Huizen NA, Coebergh van den Braak RRJ, Doukas M, Dekker LJM, IJzermans JNM, Luider TM. Up-regulation of collagen proteins in colorectal liver metastasis compared with normal liver tissue. *J Biol Chem*. 2019;294(1):281-289. https://doi.org/10.1074/jbc.RA118.005087

42. Troiani T, Martinelli E, Morgillo F, et al. Targeted approach to metastatic colorectal cancer: what comes beyond epidermal growth factor receptor antibodies and bevacizumab? *Ther Adv Med Oncol*. 2013;5(1):51-72. https://doi.org/10.1177/1758834012462462

43. Achour B, al-Majdoub ZM, Grybos-Gajniak A, et al. Liquid Biopsy Enables Quantification of the Abundance and Interindividual Variability of Hepatic Enzymes and Transporters. *Clin Pharmacol Ther*. 2021;109(1):222-232. https://doi.org/10.1002/cpt.2102

44. Zappavigna S, Cossu AM, Grimaldi A, et al. Anti-Inflammatory Drugs as Anticancer Agents. *Int J Mol Sci*. 2020;21(7):2605. https://doi.org/10.3390/ijms21072605

45. Schwenger E, Reddy VP, Moorthy G, et al. Harnessing Meta-analysis to Refine an Oncology Patient Population for Physiology-Based Pharmacokinetic Modeling of Drugs. *Clin Pharmacol Ther*. 2018;103(2):271-280. https://doi.org/10.1002/cpt.917

46. Piotrovsky VK, Huang ML, Van Peer A, Langenaecken C. Effects of demographic variables on vorozole pharmacokinetics in healthy volunteers and in breast cancer patients. *Cancer Chemother Pharmacol*. 1998;42(3):221-228. https://doi.org/10.1007/s002800050808

47. Houk BE, Bello CL, Kang D, Amantea M. A population pharmacokinetic meta-analysis of sunitinib malate (SU11248) and its primary metabolite (SU12662) in healthy volunteers and oncology patients. *Clin Cancer Res*. 2009;15(7):2497-2506. https://doi.org/10.1158/1078-0432.CCR-08-1893

48. Hudachek SF, Gustafson DL. Physiologically based pharmacokinetic model of lapatinib developed in mice and scaled to humans. *J Pharmacokinet Pharmacodyn*. 2013;40(2):157-176. https://doi.org/10.1007/s10928-012-9295-8

SUPPORTING INFORMATION

Additional supporting information may be found in the online version of the article at the publisher's website.